Scholars Journal of Engineering and Technology

OPEN ACCESS

Abbreviated Key Title: Sch J Eng Tech
ISSN 2347-9523 (Print) | ISSN 2321-435X (Online)
Journal homepage: http://saspublisher.com/sjet/

Numerical Simulations of Flow field in a Duct with Finite Rate Chemistry

R.C Mehta[1*], P. Anoop[2]

[1]Department of Aeronautical Engineering Noorul Islam Centre for Higher Education, Noorul Islam University Kumaracoil, Tamil Nadu, India
[2]Trivandrum College of Engineering Vikram Sarabhai Space Centre Trivandrum, India

***Corresponding author:** R.C Mehta

| **Received:** 05.04.2019 | **Accepted:** 10.04.2019 | **Published:** 30.04.2019
DOI: 10.21276/sjet.2019.7.4.3

Abstract | **Original Research Article**

For the past two decades, supersonic combustion ramjets and scramjets have received considerable attention to evaluate its performance employing numerical and experimental techniques. One area of active interest is the numerical simulation of chemically reacting flows where the chemical time scales can be same as or very different from fluid time scales. Such a range of time scales, referred to as stiffness, can create computational difficulties. This feature is particularly prevalent in the flame holder region of scramjet engine. Stiffness in the system of governing chemically reacting flows typically arises from the source terms in the equations describing the production and loss of the chemical species. Large values for these source terms are producing rapid changes in the dependent variables. The stiff source terms in the system of equations governing chemically reacting flow evaluated implicitly. Therefore, source terms are written implicitly at the new time level in the integration time-step. Other terms in the governing fluid dynamics equations that do not lead to stiffness are evaluated explicitly. Four inlet ramp angles are considered in present numerical simulation. The influence of the ramp angle on pressure and temperature are investigated for inlet Mach number 2.5. The aim of the present paper is to numerically analyze supersonic combustion flowfield involving chemical reaction between injecting hydrogen and a supersonic surrounding.

Keywords: Decades, ramjets, scramjets, numerical simulation, stiff source.

INTRODUCTION

The supersonic combustion in ramjets and scramjets has been studied in order to employ for hypersonic flight within the atmosphere. The basic concept being developed uses a fixed geometry modular approach that integrates with typical sounding rocket [1] to test a scramjet. The design of air-breathing hypersonic vehicles has an integrated airframe and scramjet propulsion system. The number of flow simulations is required to design scramjet inlet configuration to satisfy mission requirements. The scramjet can give unique performance at Mach 5 as compared to air breathing thermodynamic cycles. At Mach 6 and above, the scramjet which is having one cycle may be able to give sufficient propulsive power for the hypersonic flight. It is observe that scramjets can work efficiently in terms of specific impulse in the Mach number range of 3.5 – 5.0. In the ramjet major loss of total pressure is due to normal shock and coupled with combustion process.

Scramjet consists of four major components such as inlet, a fuel injector/flame holder, a combustor and a nozzle. In the injector/fuel holder region, Evans, Schexnayder and Beach [2] indicated strong coupling between finite rate chemistry and fluid dynamics. The dimension of the fuel injection point to the position of ignition temperature has important role in the combustion processes.

Drummond *et al.* [3] has employed numerical scheme to analyze the combustion problem in the injector region. In the combustion zone, the flow may be in the dual mode concepts (subsonic/supersonic) as mentioned by Breach. The diffusion time is in order of 10^{-3} – 1.0 s whereas the chemical reaction time is in order of 10^{-12} s. The system of partial differential equations describing the chemical reacting flows is stiff because of the highly disparate time scales that exit among the equations. Certain chemical reactions in the overall combustor kinetic system can take place on an extremely short time scale of 10^{-12} s, whereas the fluid dynamics may require 10^{-4} – 1.0 *s* for a typical case to reach steady-state condition.

Numerical simulation of supersonic flow through a two-strut scramjet inlet configuration has been carried out by Kumar [4, 5]. Computation schemes to address shock wave interaction in chemically reacting flow [6] has been analyzed by resolving various length and time scales in flow solver. A numerical analysis has been presented by Eklund et al. [7] to investigate the effects of combustor scale model, with different expansion angle and the length of the constant area combustor section on the mixing and combustion within a supersonic combustor. Bussing and Murman [8] have developed a finite volume method with implicit treatments of the chemically source term with point implicit multiple grid accelerator. Boiender and Doman [9] have analyzed a model for an air-breathing hypersonic vehicle employing number of complex interactions between propulsion system, aerodynamics, and structural dynamics. Northam *et al*. [10] carried out experimental and theoretical studies to determine mixing in scramjet combustors using parallel fuel injection from the base of swept and unswept wall mounted ramps.

One area of active interest is the computation of chemically reacting flows where the chemical time scales can be same as or very different from the fluid time scales. Such a range of time scales, referred to as stiffness, can create major computational difficulties. This feature is particular prevalent in the flame holder region of scramjet. The point-implicit scheme treats the convection and diffusion terms explicitly and source term implicitly. This leads to a pre-conditioner, which effectively removes the chemical time scale limitations of explicit numerical schemes. The main of the present paper is to numerically simulate supersonic combustor flow fields involving chemical reaction between injected hydrogen and a supersonic external field.

Governing equations

The flow model is two dimensional, inviscid, finite rate chemical reacting multi-species. Two-steps chemical reaction is taking place and neglecting effect of density perturbation. Inlet air is parallel to the combustor wall. The chemical reaction of hydrogen and oxygen is modeled in the present paper with the global finite-rate hydrogen-air chemistry model of Roger and Chiniz [11]. This model adequately represents the chemical reaction taking place in the problems to be considered, and it also produces an extremely large disparity in the time scales present in the problems. This phenomenon allows the ability of the numerical algorithm to deal with resulting stiffness of finite rate reaction equation.

The governing time-dependent two-dimensional compressible Euler equations with finite rate chemistry can be written in the following conservation form

$$\frac{\partial \boldsymbol{U}}{\partial t} + \frac{\partial \boldsymbol{E}}{\partial x} + \frac{\partial \boldsymbol{F}}{\partial y} + H = 0 \qquad (1)$$

where

$$\boldsymbol{U} = r\begin{bmatrix}\rho\\ \rho u\\ \rho v\\ \rho e\\ \rho Y_i\end{bmatrix}, \qquad \boldsymbol{E} = \begin{bmatrix}\rho u\\ \rho u^2 + p\\ \rho uv\\ (\rho e + p)u\\ \rho Y_i\, u\end{bmatrix} i, \qquad \boldsymbol{F} = \begin{bmatrix}\rho v\\ \rho uv\\ \rho v^2 + p\\ (\rho e + p)v\\ \rho Y_i\, v\end{bmatrix}, \quad H = \begin{bmatrix}0\\ 0\\ 0\\ 0\\ -\dot{\omega}\end{bmatrix}$$

$\boldsymbol{U}$ is the state vector, $\boldsymbol{E}$ and $\boldsymbol{F}$ are inviscid flux and $\boldsymbol{H}$ is source vector. Y_i is the j^{th} density fraction and ω_i is the chemical source term. The total specific energy and temperature is related to pressure and density by the perfect gas equation of state as

$$e = \sum_{j=1}^{N_s} \int Y_j C_{vj} dT + \frac{1}{2}(u^2 + v^2) + \sum y_i H_{fi}$$

$$p = \rho R^0 T \sum_{j=1}^{N_s} \left(\frac{Y_i}{w_i}\right)$$

where H_{fi} is the heat of formation for species, N_s is the number of species and w_j is the molecular weight of species. R^0 is universal gas constant.

Numerical scheme

To facilitate the spatial discretization in the numerical scheme, the governing equations (1) can be written in the integral form over a finite volume as

$$\frac{\partial}{\partial t}\int_{\Omega} \boldsymbol{U} d\Omega + \int_{\Gamma}(\boldsymbol{E}dy - \boldsymbol{G}dx) - \int_{\Omega} \boldsymbol{H} d\Omega = 0 \qquad (2)$$

where Ω is the computational domain, Γ is the boundary domain. The contour integration around the boundary of the cell is divided in the anticlockwise sense.

The computational domain is divided into a finite number of non-overlapping quadrilateral grids. The conservation variables within the computational cell are represented by their average values at the cell centre. When the integral governing equation (2) is applied separately to each cell in the computational domain, we obtain a set of coupled ordinary differential equation of the form

$$A_{i,j}\frac{dU_{ij}}{dt} + Q(\boldsymbol{U}_{i,j}) - D(\boldsymbol{U}_{i,j}) + A_{i,j}(\boldsymbol{H}_{i,j}) = 0 \qquad (3)$$

where $A_{i,j}$ is the area of the computational cell, $Q(\boldsymbol{U}_{i,j})$ is the inviscid and $D(\boldsymbol{U}_{i,j})$ is the artificial dissipation flux added for numerical stability.

Inviscid terms

The convective fluxes are calculated at the centre of the grid, resulting in cell-centre flux balances. The contour integration of the inviscid flux vector is approximated as

$$Q(\boldsymbol{U}_{i,j}) = \sum_{s=1}^{4}(\boldsymbol{E}_s \Delta y_s - \boldsymbol{F}_s \Delta x_s) \qquad (4)$$

where *s* is the side of the computational grid. The summation is carried out over the four edges of the grid.

Artificial dissipation

In the cell-centered spatial discretization schemes, such as the one described above which is non-dissipative, therefore, artificial dissipation terms are added to Eq. (3). The approach of Jameson *et al.* [12] is adopted to construct the dissipative terms $\boldsymbol{D}_{ij}$ consisting of blend of second and fourth differences of the vector conserved variables $\boldsymbol{U}_{ij}$. Fourth differences are added everywhere in the flow domain where the solution is smooth, but are 'switched off' in the region of shock waves. A term involving second differences is then 'switched on' to damp oscillations near shock waves. This switching is achieved by means of a shock sensor based on the local second differences of pressure. Since the computational domain is structured, the cell centers are defined by two indices (i, j) in these coordinate directions. The dissipation terms are written in terms of differences of cell-edge values as

$$\boldsymbol{D}_{i,j} = \frac{\Delta A_{i,j}\,(d_{AB} - d_{CD} + d_{BC} - d_{DA})}{\Delta t_{i,j}} \qquad (5)$$

where $\Delta t_{i,j}$ is the local cell centre time step. The cell-edge components of the artificial dissipation terms are composed of first and third differences of dependent, e.g.

$$d_{AB} = d_{AB}^{(2)} - d_{AB}^{(4)}$$

with

$$d_{AB}^{(2)} = \epsilon_2^{(2)}(\boldsymbol{U}_{i+1,j} - \boldsymbol{U}_{i,j})$$

$$d_{AB}^{(4)} = \epsilon_2^{(4)}(\boldsymbol{U}_{i+2,j} - 3\boldsymbol{U}_{i+1,j} + 3\boldsymbol{U}_{i,j} - \boldsymbol{U}_{i-1,j})$$

The adaptive coefficients are

$$\epsilon_2^{(2)} = \kappa^{(2)} \max(\upsilon_{i+1,j}, \upsilon_{i,j})$$

$$\epsilon_2^{(4)} = \max(0, \kappa^{(4)} - \epsilon_2^{(2)})$$

are switched on or off by use of the shock wave sensorν, with

$$\nu_{i,j} = \left|\frac{p_{i+1,j} - 2p_{i,j} + p_{i-1,j}}{p_{i+1,j} + 2p_{i,j} + p_{i-1,j}}\right|$$

where $\kappa^{(2)}$ and $\kappa^{(4)}$ are constants, taken equal to 0.25 and 0.003906 respectively in the above calculations. The scaling quantity $(\Delta A/\Delta t)_{i,j}$ in the above confirms the inclusion of the cell volume in the dependent variable. The blend of second and fourth differences provides third-order back ground dissipation in smooth region of the flow and first-order dissipation in shock waves.

Time marching scheme

The spatial discretization described above reduces the governing flow equations to semi-discrete ordinary differential equations. The integration is performed employing an efficient multistage scheme [12]. The following three-stage, time-stepping method is adapted for the present work (neglecting for clarity, the subscripts *i* and *j*)

$$\begin{aligned} \boldsymbol{U}^{(0)} &= \boldsymbol{U}^{n} \\ \boldsymbol{U}^{(1)} &= \boldsymbol{U}^{n} - 0.6\Delta t\left(Res^{(0)} - \boldsymbol{D}^{(0)}\right) \\ \boldsymbol{U}^{(2)} &= \boldsymbol{U}^{n} - 0.6\Delta t\left(Res^{(1)} - \boldsymbol{D}^{(0)}\right) \\ \boldsymbol{U}^{(3)} &= \boldsymbol{U}^{n} - 1.0\Delta t\left(Res^{(2)} - \boldsymbol{D}^{(0)}\right) \\ \boldsymbol{U}^{n+1} &= \boldsymbol{U}^{(3)} \end{aligned} \tag{6}$$

where *n* is the current time level, *n*+1 is the new time level, the residual Res is the sum of the inviscid fluxes. In order to minimize the computation time, the expensive evaluation of the dissipative terms $\boldsymbol{D}$ is carried out only at the first intermediate stage (*0*) and then frozen for the subsequent stages. A conservative choice of the Courant-Friedritchs-Lewy number (1.4) was made to achieve a stable numerical solution. The numerical algorithm is second-order accurate in space and time discretization.

Time rescaling

The steady state solution is desired then the time history can be modified to remove the chemical time scales. The fluid and species quantity could be marched together in pseudo time, then the fast processes which require time steps small time step would not hold up the slower processes which could be marched at larger time steps. It turns out that the governing equations can be modified to reflect this desired pseudo time behavior by rewriting them as

$$S\frac{\partial \boldsymbol{U}}{\partial t} = -\frac{\partial \boldsymbol{E}}{\partial x} - \frac{\partial \boldsymbol{F}}{\partial y} - H \tag{7}$$

where *S* is a pre-conditioning matrix whose purpose is to normalize the various time scales to be the same order.

Derivative of scaling matrix

The stiffness can be defined as the ratio of the largest eigenvalue to the smallest eigenvalue of the Jacobians to the flux vectors in the governing equation (1). In the case of reacting flows, the stiffness is the source terms in the species conservation equations. In the case of problem involving large number of species, several chemical time scales occur and they are to be compared with the fluid dynamics time scale.

As mentioned above the *S* matrix can take on a variety of forms to determine the forms of the *S* matrix and specifically what the matrix elements should contain, considering the following. If the time stiffness is to be removed from the problem then the matrix *S* should in some way contain the chemical time scales. The desired time scale character can be seen by considering the species equation without conservation term, i.e.,

$$\frac{dU_y}{dt} = -H = -\frac{kU_y}{\rho} \tag{8}$$

Integrating the above equation yields

$$U_y = Ce^{\left(-\frac{kt}{\rho}\right)} = Ce^{\left(-\frac{1}{\tau_{chem}}\right)}$$

where τ_{chem} is characteristic time scale = ρ/k. Thus, U_y equation is dependent on τ_{chem} through the exponential term. Now differentiating *H* with respect to U_y as

$$\frac{dH}{dU_y} = \frac{1}{\tau_{chem}}$$

This derivative is also related the chemical time scale, τ_{chem}. This would suggest the spectral should contain element like *dH*/*dU*. It should be pointed out that the derivative *dH*/*dU* for a system of equation becomes Jacobian.

In the point implicit method where the spatial gradient terms treated explicitly and the chemical source term are treated implicitly. The point implicit scheme can be written as

$$\frac{U^{n+1}-U^n}{\Delta t} = -\left(\frac{\partial E}{\partial x}\right)^n - H^{n+1} \qquad (9)$$

to solve this equation H^{n+1} is be linearized using Newton method.

Chemical reaction model

The chemical reaction of hydrogen and oxygen is modelled using the global finite rate hydrogen air chemistry model of Roger and Chinitz [11]. This model adequately represents the chemical reaction taking place in the problems to be considered, and it also produces an extremely large disparity in the time scales present in the problems. This phenomenon allows the ability of the numerical algorithm to deal with resulting stiffness to be demonstrated.

The Roger and Chinitz model assume that the overall reaction of hydrogen and oxygen takes place though two reactions, the first resulting in the formation of a hydroxyl radical and the second combining the hydroxyl radical with hydroxy to form water.

$$\begin{aligned} H_2 &\underset{K_{b1}}{\overset{K_{f1}}{\rightleftharpoons}} 2OH \\ 2OH &\underset{K_{b2}}{\overset{K_{f2}}{\rightleftharpoons}} 2H_2O \end{aligned} \qquad (10)$$

It is important to say that nitrogen is present in the calculation but is assumed inert. So four species are H_2, O_2, H_2O, N_2. The K_f values are forward reaction rates and K_b values are reverse reaction rates. The reverse rates can be found, given the forward and the equilibrium constant K for each reaction as

$$K_b = \frac{K_f}{K}$$

The forward reaction rate is computed from Arrhenius law as

$$K_{f1} = A_i(f)T^{N_i}e^{(E_i/R^0T)} \qquad (11)$$

For each i, and here there are 8 reaction finite rates.

Table-1: Values of constant in the finite rate reaction equation

i	Reaction	A	N	E
1	$OH + O = H + O_2$	3.0 E –11	0.0	0.96
2	$OH + O = H_2 + O$	1.4 E –14	–1.0	0.7
3	$OH + OH = H_2O + O$	1.0 E –11	0.0	1.1
4	$OH + H_2 = H_2O + H$	3.5 E –11	0.0	5.18
5	$2H + N_2 = H_2 + N_2$	3.0 E –30	1.0	0.0
6	$H + O + N_2 = OH + N_2$	1.0 E –29	1.0	0.0
7	$2O + N_2 = O_2 + N_2$	3.0 E –34	0.0	– 1.8
8	$H + OH + N_2 = H_2 + N_2$	1.0 E –25	2.0	0.0

Boundary and initial conditions

The flow variables at the inflow boundary are held fixed at given freestream values. At the inlet pressure, temperature and Mach number are 1.01×10^5 Pa, 900^0 K and 2.5 respectively. An extrapolation from the interior grid points is used to obtain the flow variables at the out-flow boundary. Slip conditions are used on the solid boundaries. On the exit boundary, extrapolation from interior grid points of the exit plane is used to compute flow variables. If the flow is symmetric about a plane, only half of the flow field is calculated and symmetry boundary conditions are imposed.

Geometry of supersonic inlet

Figure 1 shows the combustor model considered for the present numerical simulations. The length L is 1.0 m and width W = 0.5 m. The ramp angle α is depicted in Fig. 1. The computation is carried out on quadrilateral grid as shown in Fig. 2. The computation is performed on 60 × 60 cells which is selected after considering the grid independent test. Since we are dealing with inviscid flow, therefore, the grid stretching is not needed in numerical algorithm. The two dimensional flow solvers are validated with oblique shock analytical expressions. The convergence criteria are based upon the difference between two successive iteration as $\left|\rho^{n+1}-\rho^{n}\right| \leq 10^{-5}$ where n is the iteration index.

RESULTS AND DISCUSSION

A supersonic inlet has been considered for the present numerical analysis. This represents a class of scramjet combustors. Eight transport equations are required to be solved. The two-dimensional code was validated by comparing it with the oblique shock wave theory. Four different ramp angles $\alpha = 5^0$, 10^0, 20^0 and 30^0) upper wall are considered to obtain pressure and temperature distributions.

Mach, density and temperature contours for $\alpha = 10^0$ ramp angles are shown in Figure 3.The contour plots show formation of ramp shock. It can also observe from the contour plots that the pressure and temperature increases downstream of the ramp shock.

For different ramp angles, upper wall pressure is shown in Fig. 4. As ramp angle increases upper wall pressure in the converging region increases. Lower wall pressure variation for different ramp angle reveals that as the ramp angle increases the maximum pressure value shift to left side as seen in Fig. 5. Upper and lower wall temperature variations along the wall are shown in Figs. 6 and 7, respectively. The temperature distribution increases with the increasing ramp angle.

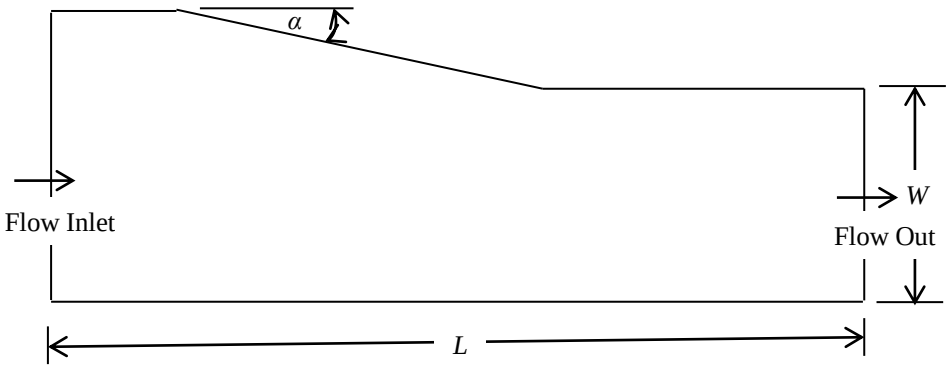

Fig-1: Geometrical parameters of the supersonic inlet

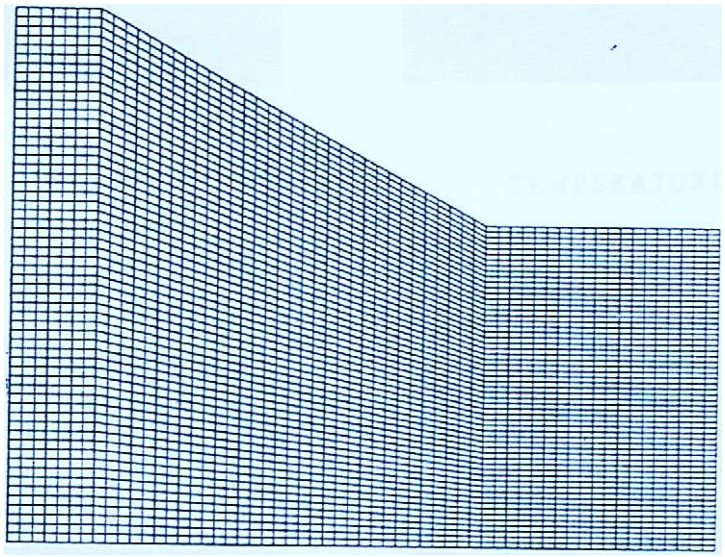

Fig-2: Computational grid in the supersonic inlet

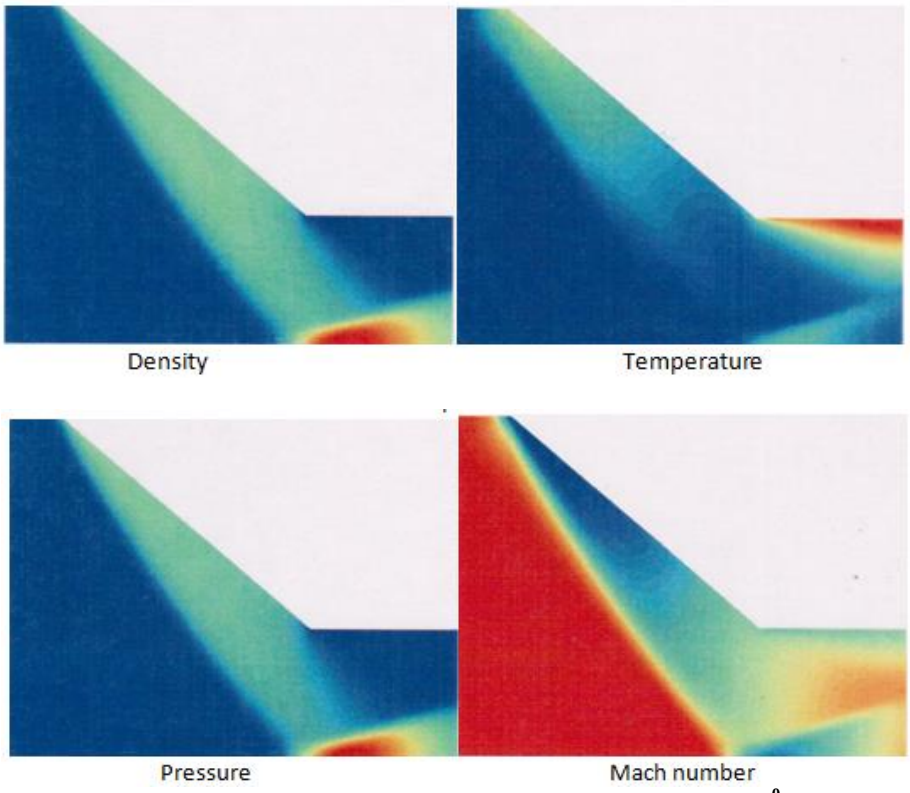

Fig-3: Contour plots inside the supersonic inlet at $\alpha = 20^0$

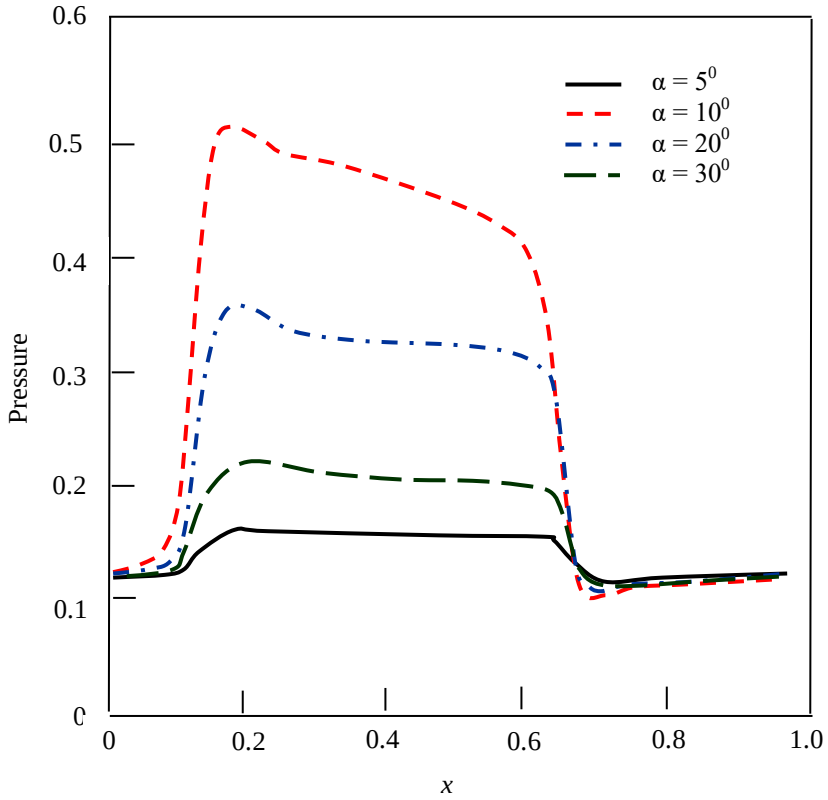

Fig-4: Variation of pressure on upper wall of the inlet

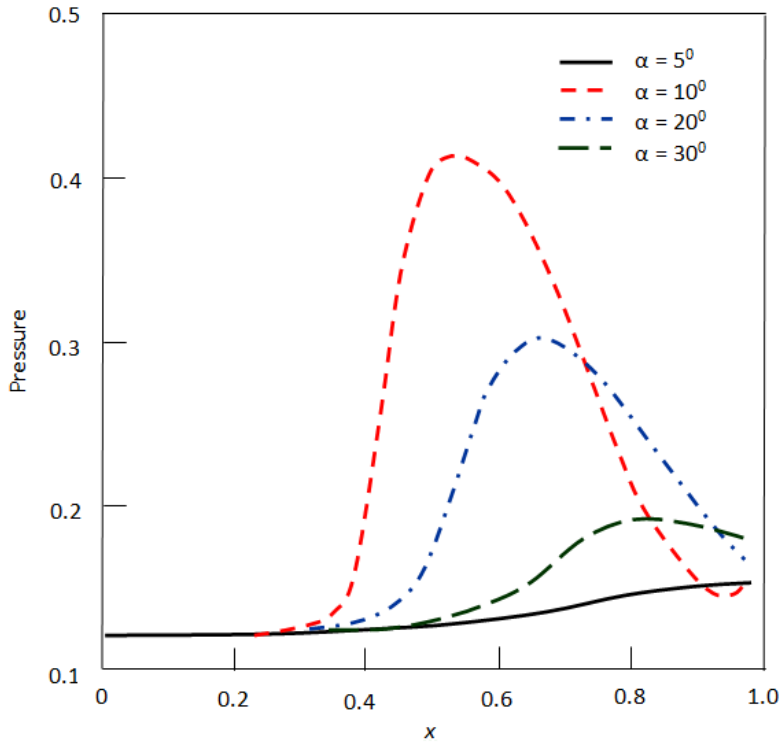

Fig-5: Variation of pressure on lower wall of the inlet

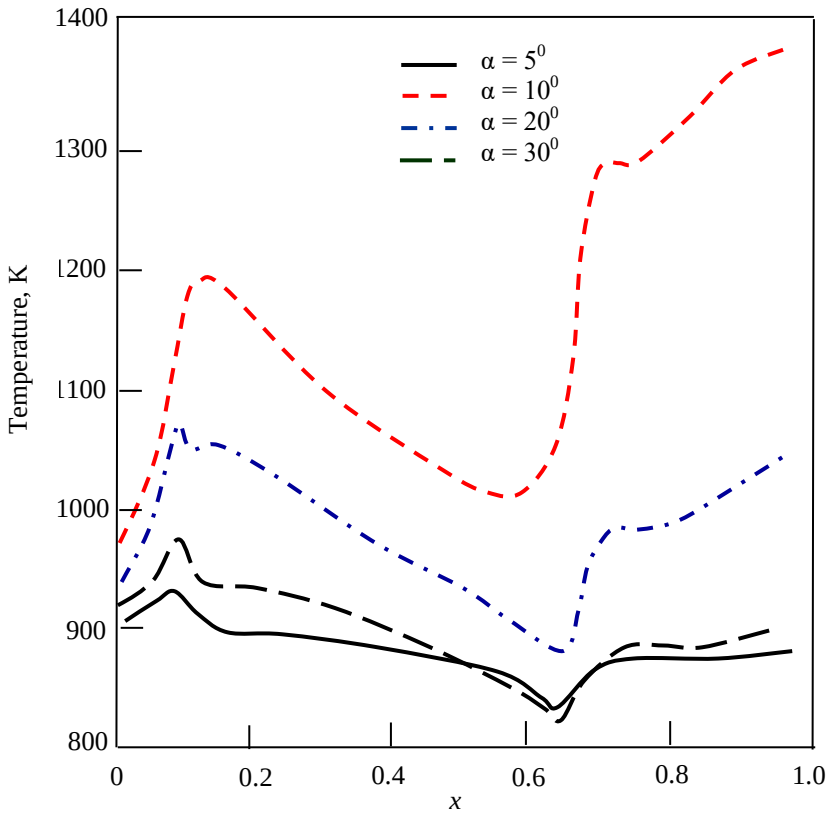

Fig-6: Variation of temperature on upper wall of the inlet

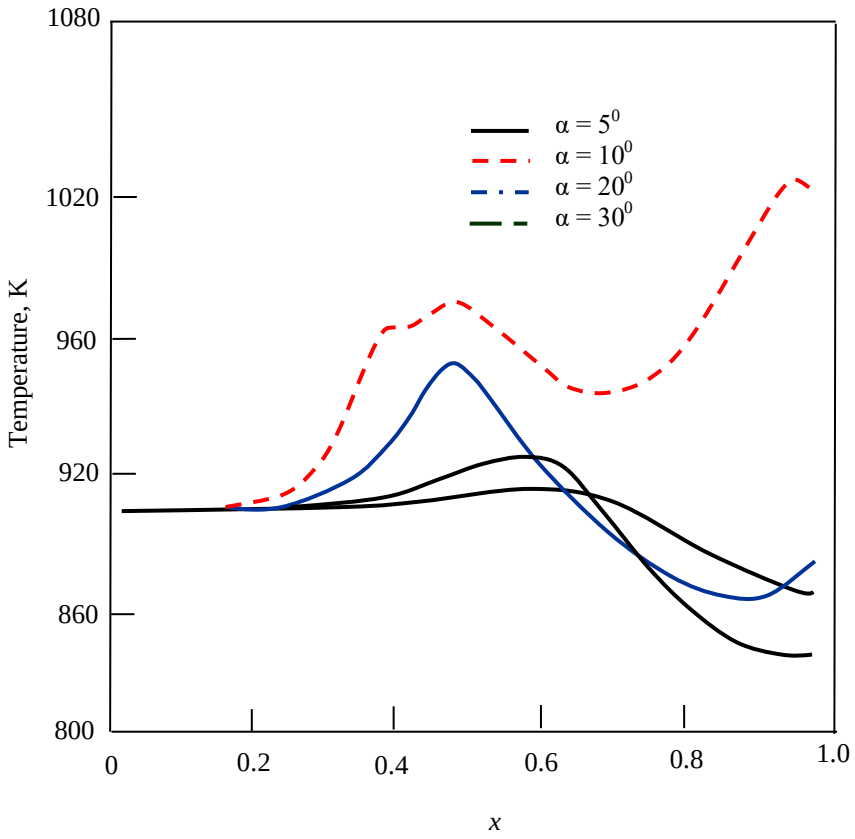

Fig-7: Variation of temperature on lower wall of the inlet

CONCLUSIONS

A point implicit method for efficiently solving flow problems with finite rate chemistry has been employed in order to find species production rate. A hydrogen-air chemistry model has been used to model non-trivial chemical reacting flows. The inlet pressure, temperature and Mach number are 1.01×10^5 Pa, 900^0 K and 2.5 respectively considered. Flow fields for different ramp angle has been discussed. It is found that the ramp shock wave becomes predominant as ramp angle increases.

REFERENCES

1. Special issue on “Scramjet flight testing”, Edited by K. Sivan in the Journal of Aerospace Sciences and technologies. 2018; 70(3A).
2. Evans JS, Schexnayder Jr CJ, Beach Jr HL. Application of a two-dimensional parabolic computer program to prediction of turbulent reacting flows.
3. Drummond JP, Hussaini MY, Zang TA. Spectral methods for modeling supersonic chemically reacting flowfields. AIAA journal. 1986 Sep;24(9):1461-7.
4. Kumar A. Numerical simulation of flow through a two-strut scramjet inlet. Journal of Propulsion and Power. 1989 May;5(3):341-5.
5. Kumar A. Numerical analysis of the scramjet inlet flow field using two-dimensional Navier-Stokes equations. In19th Aerospace Sciences Meeting. 1981:185.
6. Chung TJ. Turbulent/shock wave interactions in chemically reacting flows, Sadhana, Part, August. 1993; 18(3;4):637-655.
7. Eklund D, Northam G. A numerical study of the effects of geometry on the performance of asupersonic combustor. In30th Aerospace Sciences Meeting and Exhibit. 1992:624.
8. Bussing TR, Murman EM. Finite-volume method for the calculation of compressible chemically reacting flows. AIAA journal. 1988 Sep;26(9):1070-8.
9. Bolender MA, Doman DB. Nonlinear longitudinal dynamical model of an air-breathing hypersonic vehicle. Journal of spacecraft and rockets. 2007 Mar;44(2):374-87.
10. Northam GB, Capriotti DP, Byington CS, Greenberg I. Mach 2 and Mach 3 mixing and combustion in scramjets.1991.
11. Rogers RC, Chinitz W. Using a global hydrogen-air combustion model in turbulent reacting flow calculations. AIAA journal. 1983 Apr;21(4):586-92.

12. Jameson A, Schmidt W, Turkel E. Numerical solution of the Euler equations by finite volume methods using Runge Kutta time stepping schemes. In14th fluid and plasma dynamics conference. 1981(23):1259.